GPS Solutions (2024) 28:25
https://doi.org/10.1007/s10291-023-01555-w

ORIGINAL ARTICLE

Galileo high accuracy service performance and anomaly mitigation capabilities

Ilaria Martini[1,3] · Melania Susi[1,4] · Luca Cucchi[1] · Ignacio Fernandez-Hernandez[2]

Received: 8 June 2023 / Accepted: 28 September 2023 / Published online: 10 November 2023
© @European Union 2023

Abstract
Precise point positioning (PPP) and real-time kinematic techniques are interesting in several sectors, especially for autonomous applications. These users have high accuracy needs coupled with stringent requirements on continuity, availability, integrity, and convergence time, whose satisfaction can be challenging in harsh environments. Galileo launched on January 2023 the initial high accuracy service (HAS), a European free-of-charge PPP service with a worldwide coverage transmitted on E6 signals and provided through an internet connection. This paper characterizes the Galileo HAS product performance, including orbital errors, clock errors, code biases, and overall signal in space error (SISE), with live signals transmitted since HAS service declaration. The paper also presents the behavior of HAS SIS in the case of four satellite anomalies between September 2021 and August 2022, occurring for Galileo and GPS. Finally, the paper presents the results of HAS performance in both static open sky and road scenarios, showing a few-decimeter accuracy even in environments with degraded visibility. The paper shows the improvements in terms of robustness to satellite anomaly thanks to the Galileo HAS characteristics.

Keywords GNSS · PPP · HAS · Integrity · Safety–critical · Satellite · Automotive

Introduction

High accuracy service (HAS) is the European free PPP service provided by Galileo. On January 24, 2023, the European Commission announced the start of its initial services. The message provides orbit, clock, code biases, and soon phase biases for Galileo E1-E5a-E5b-E6 and GPS L1C/A-L2C signals. The message corrects the Galileo I/NAV and GPS LNAV L1 C/A combinations and is transmitted in the Galileo E6 signal (E6-B data component) and through the Galileo HAS internet data distribution (IDD).

Although HAS service does not provide an integrity commitment, safety–critical users may take benefit by exploiting it in evolutions of receiver autonomous integrity monitoring algorithm (RAIM) (Blanch et al. 2012; Gunning et al. 2018; Crespillo et al. 2023). The receiver can in fact closely monitor the dynamic of the error over time and react if necessary. The HAS real-time capability implies that there is only a few-second delay between the generation of the corrections and their provision to the user. The service also provides status information if a specific satellite shall not be used allowing to reduce the time in which the user is affected by the faults. In the future signal quality indicators will be provided and further enhance the integrity bounds estimation.

Galileo HAS overview

The service is being provided in two phases, where phase 1 encompasses the initial service provision and phase 2 the full-service provision. Phase 1 includes only the so-called service level 1 (SL1), with corrections for Galileo E1/E5b/E5a/E6 and GPS L1/ L2C signals. SL1 performance targets

✉ Luca Cucchi
Luca.Cucchi@ec.europa.eu

Ilaria Martini
Ilaria.Martini@u-blox.com

Melania Susi
msusi@topcon.com

Ignacio Fernandez-Hernandez
Ignacio.Fernandez-Hernandez@ec.europa.eu

[1] European Commission, Joint Research Centre (JRC), Ispra, Italy

[2] European Commission, DG DEFIS, Brussels, Belgium

[3] Present Address: U-Blox, Sgonico, Italy

[4] Present Address: Topcon Positioning System, Modena, Italy

are 20/40 cm (95%) for the horizontal/vertical precision and a maximum convergence time of 300 s. Service level 2 (SL2) will be part of phase 2 and will additionally offer corrections for Galileo E5, GPS L5, atmospheric corrections and signal quality indicators over the European coverage area (ECA) with a maximum convergence time of 100 s (European Union Space Program Agency (EUSPA) 2020).

Galileo HAS is transmitted in the C/NAV pages of the E6-B signal component at a carrier frequency of 1278.75 MHz and at a maximum rate of 448 bits per second (bps) (European Union Space Program Agency (EUSPA) 2022a, b, c). C/NAV pages are encoded though a so-called high-parity vertical reed-Solomon (HPVRS) scheme, to facilitate reception (Fernandez-Hernandez et al. 2020). HAS is broadcast from a subset of satellites, currently up to 20. Each C/NAV page is transmitted every second and contains HAS messages with the following possible blocks: Mask, Orbit Corrections, Clock Full-Set Corrections, Clock Subset Corrections, Code Biases, and Phase Biases. Currently, a message is transmitted with the Mask, Orbit, and Biases blocks every 50 s, while another message with the Clock Full-Set block is transmitted every 10 s. As it will be shown later, the high update rate of the clocks allows to closely follow rapid changes of the ranging error.

In the HAS orbit corrections, the minimum value indicates that the HAS corrections are not available, and the satellite shall not be used (− 10.2375 m for the radial correction and − 16.376 m for the In-Track and Cross-Track corrections). In the HAS clock correction, the minimum value (− 10.2375 m) informs the user that the data are not available, while the maximum ones (10.2375 m) inform that the satellite shall not be used. These functionalities are important when an anomaly occurs in the HAS provision or in the satellite itself to inform users and reduce their exposure to the anomaly.

The Galileo HAS corrections currently are based on an orbit determination and time synchronization (ODTS) algorithm running every 30 min using 3-day data arcs and a sequential clock estimation (Fernandez-Hernandez et al. 2022). The Code Biases Block contains the Code biases (− 20.46 indicates data not available), and the Phase Biases Block contains the Phase biases (− 10.23 indicates data not available) and the Phase Discontinuity Indicator, which is a counter, incremented every time a phase discontinuity is detected.

The HAS corrections are transmitted also through a ground dissemination channel, Galileo HAS Internet Data Distribution (IDD), based on an NTRIP protocol in a RTCM-like format (RTCM Standard 10410.1, January 12 2021; (RTCM Standard 10403.3, May 20 2021)). Users get access to it through the Galileo Service Centre (GSC) (European Union Space Program Agency 2023a; b). The Galileo HAS internet data distribution interface control document (IDD ICD), available to registered users, describes the correction format, fully equivalent to the broadcast ones. A client application allows to access the internet stream (e.g., open-source NTRIP client of the Federal Agency for Cartography and Geodesy, Bundesamt für Kartographie und Geodäsie (BKG)).

The next section characterizes the Galileo HAS product performance with live signals transmitted since HAS service declaration. Later, the paper presents the behavior of HAS SIS in the case of four satellite anomalies between September 2021 and August 2022, occurring for Galileo and GPS. Then, the paper presents the results of HAS users in both static open sky and road scenarios, both performed at the JRC premises in Ispra, Italy. Finally, the paper presents some conclusions.

Galileo HAS product performance

This section presents the Galileo HAS product performance, including the satellite orbit errors (Radial, In-Track, Cross-Track), clock errors, group delay biases, and signal in space error (SISE). The analysis compares the HAS correction errors with the errors in the Galileo and GPS broadcast navigation message. It also covers probability density functions and cumulative density functions down to low probabilities, which is relevant for users with safety requirements, in particular those users requiring to bound the distribution tails.

The signal in space error (SISE) was analyzed by comparing broadcast and corrected orbit and clocks to reference products of the Center for Orbit Determination in Europe (CODE), which provided the best availability during the specific anomalies observed. The latter ones were adjusted to the Antenna Phase Center using the latest IGS reference antenna offsets file (igs20.atx dated 2 October 2022) (Teunissen and Montenbruck 2017).

The SISE analytical was derived from the in-track (x_{IT}), cross-track (x_{CT}) and radial (x_R) orbit error components and the clock error (δt_{CLK}) using the following equation

$$\mathrm{SISE}_i = \sqrt{0.9610 \cdot x_R^2 + \delta t_{CLK}^2 + 0.01545 \cdot \left(x_{IT}^2 + x_{CT}^2\right) + 1.96881 \cdot \delta t_{CLK} \cdot x_R} \quad (1)$$

which is specified in the Galileo Open Service Definition (European Union Space Program Agency 2019) and corresponds to the average SISE in satellite coverage area.

The satellite biases affecting the ranging errors were also analyzed. These errors are caused by differences in the satellite processing of the signals among the different frequencies, or signal deformation due to no linearities of the satellite transfer function. The errors in the broadcast satellite group delays (i.e., Broadcast Group Delays for Galileo and

Time Group Delay for GPS) were computed and compared with the HAS corrections (i.e., Code Biases).

Differential Code Bias (DCB) of the DLR products (C1X-C7X combination) were used as reference. The Galileo Broadcast Group Delays (BGD) were scaled with a frequency-dependent scaling factor using the following equation

$$\Delta b_{\text{Galileo}} = \frac{\text{BGD}_{\text{E1E5b}}}{k_{\text{E1E5b}}} - \text{DCB}_{\text{C1X-C7X}} \tag{2}$$

$$k_{\text{E1E5b}} = \frac{f_{\text{E5b}}^2}{\left(f_{\text{E5b}}^2 - f_{\text{E1}}^2\right)} \tag{3}$$

which compares the BGD to the DCB and assesses their differences (Martini et al. 2022).

The DLR DCB combinations were selected by choosing the combination closest to the E1-E5b and L1-L2 frequencies considering that not all the DCB combinations are available in the IGS reference files Document (Montenbruck et al. 2018). For GPS the LNAV time group delay (TGD), the group delay between L1 P(Y) and L2 P(Y) signals, was compared to the C1C-C2W DCB after the application of the proper scaling factor

$$\Delta b_{\text{GPS}} = \frac{\text{TGD}_{\text{L1L2}}}{k_{\text{L1L2}}} - \text{DCB}_{\text{C1C-C2W}} \tag{4}$$

$$k_{\text{L1L2}} = \frac{f_{L2}^2}{\left(f_{\text{L2}}^2 - f_{\text{L1}}^2\right)} \tag{5}$$

accordingly, to equations described in Martini et al. (2022).

Minor differences between the HAS generation process and the IGS one were taken into account in the processing. The HAS clock corrections refer to E1C-L2P dual-frequency combination, while IGS reference products refer to L1P-L2P combination. In addition, the HAS corrections refer to the Galileo System Time, while IGS products refer to GPS one. To handle these differences the mean of the clock errors over the constellation at each instant of time was removed, while for the orbit component, the mean over time for each satellite for the radial component was removed, since these error components are absorbed by the user clock error.

HAS live corrections have been collected from the SIS at the European Commission Joint Research Centre (JRC) in Ispra, Italy, since the first live signals in May 2021. However, the data analyzed in this work span between January 28 and February 4, 2023, following the period after service declaration. Only epochs with both broadcast and corrections available were considered. A high-performance geodetic Trimble Zephyr 2 antenna on the rooftop of the laboratory was connected to a Septentrio PolaRx5S receiver.

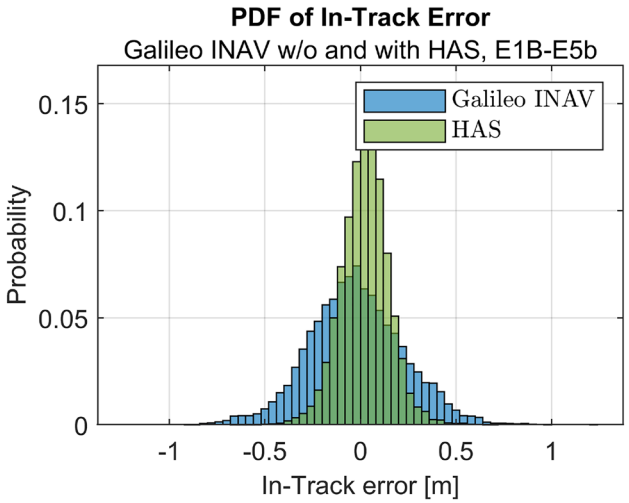


Fig. 1 Improvement of orbit errors when applying HAS, in particular the figure shows the PDF of Galileo In-Track error without (blue) and with HAS (green)

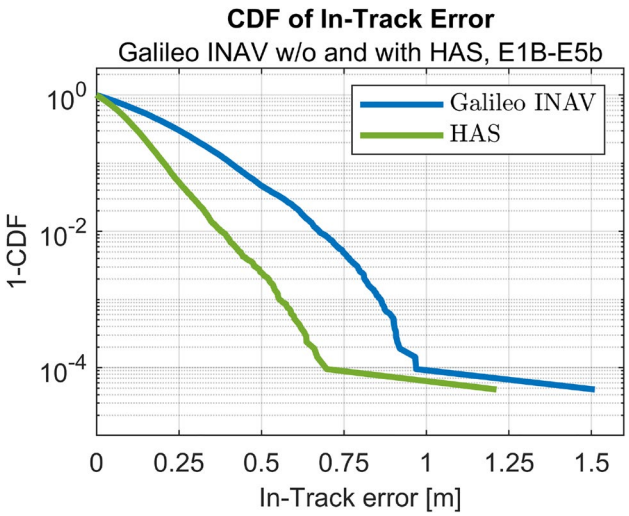


Fig. 2 Improvement of orbit errors when applying HAS, in particular the figure shows the 1-CDF of Galileo In-Track error without (blue) and with HAS (green)

Data included only C/NAV pages with CRC passed, and a decoder of the message was developed in-house and validated against reference HAS data uploaded to the Galileo satellites and against independent decoder implementations HASlib (Horst et al. 2022).

Satellite orbit error

Satellite orbit errors were characterized first per component (In-Track, Cross-Track, and Radial).

Figures 1, 2, 3, 4, 5, and 6 show the results for Galileo I/NAV and Figs. 7, 8, 9, 10, 11, and 12 GPS LNAV.

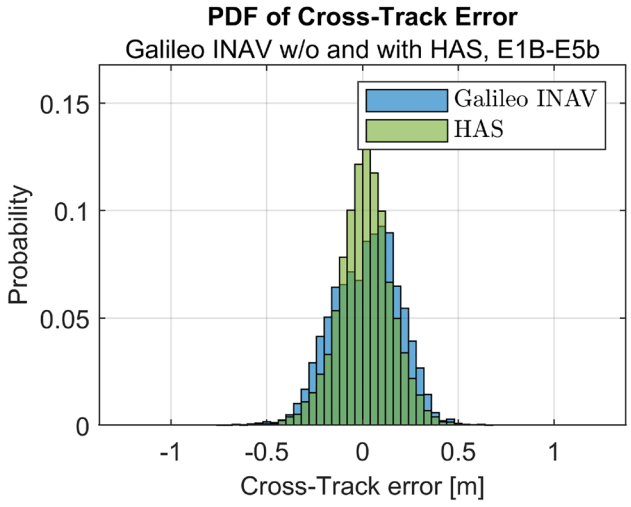


Fig. 3 Improvement of orbit errors when applying HAS, in particular the figure shows the PDF of Galileo Cross-Track error without (blue) and with HAS (green)

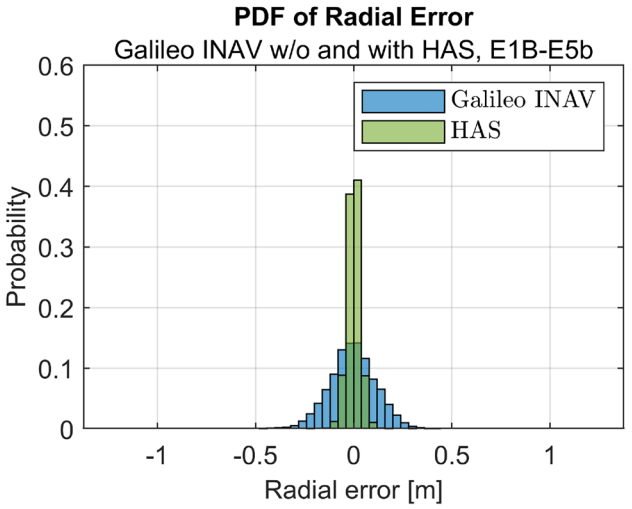


Fig. 5 Improvement of orbit errors when applying HAS, in particular the figure shows PDF of Galileo Radial error without (blue) and with HAS (green)

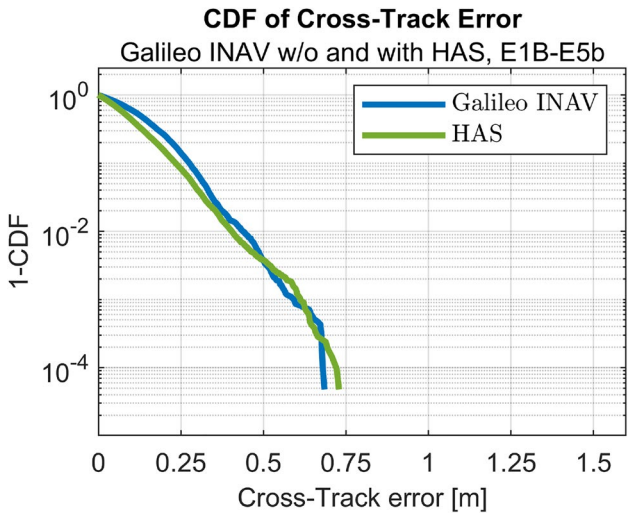


Fig. 4 Improvement of orbit errors when applying HAS, in particular the figure shows 1-CDF of Galileo Cross-Track error without (blue) and with HAS (green)

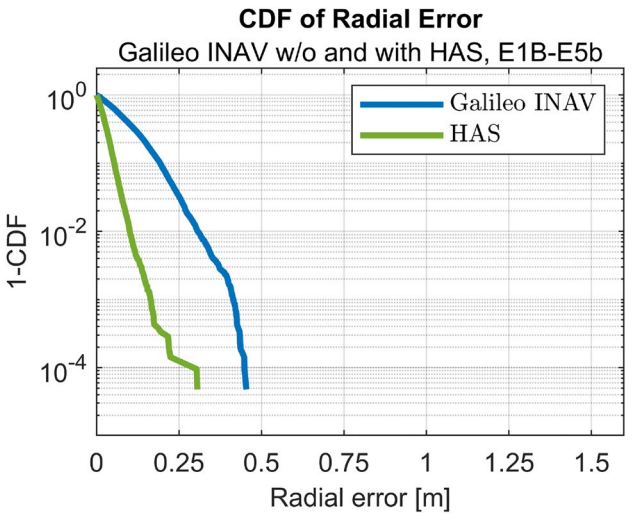


Fig. 6 Improvement of orbit errors when applying HAS, in particular the figure shows 1-CDF of Galileo Radial error without (blue) and with HAS (green)

Data from all satellites in each constellation were combined in a single distribution to maximize the statistical confidence of the results. On the left side, the probability density function (PDF) is represented for the broadcast navigation message (blue) and for the message corrected by HAS (green). The probability was assessed using the empirical histogram of the sample data. On the right side, the one-side cumulative density function (CDF) of the same empirical data is represented. One-side cumulative distribution function is the distribution of the absolute value of the error component. The experimentation duration allowed reaching a probability of 5×10^{-5}. The legend of each figure shows the mean and root-mean-square of each component.

Figures 1, 2, 3, 4, 5, and 6 show that after applying HAS corrections, the Galileo orbit errors improved and they reduced by a factor 2 for the In-Track, 1.2 for the Cross-Track, and 3.4 for the Radial. The Cross-Track component presents a slight degradation at the end of the distribution for smaller probability, which is related to probabilities difficult to be estimated over the short observation period considered and are expected to disappear when more data will be collected and used for the characterization. The

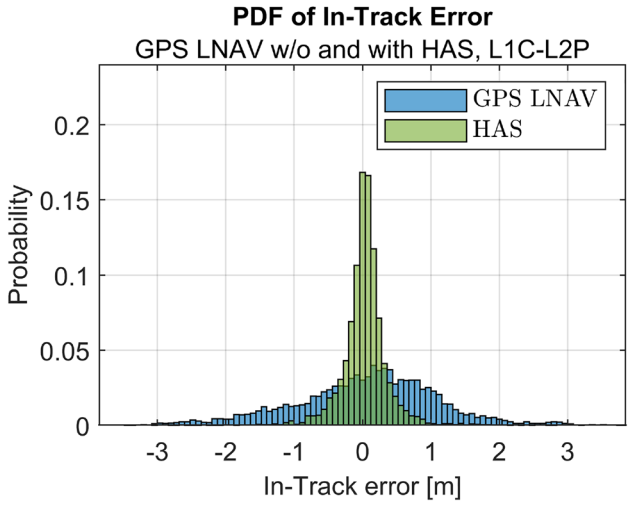


Fig. 7 Improvement of orbit errors when applying HAS, in particular the figure shows PDF of GPS ln-Track error without (blue) and with HAS (green)

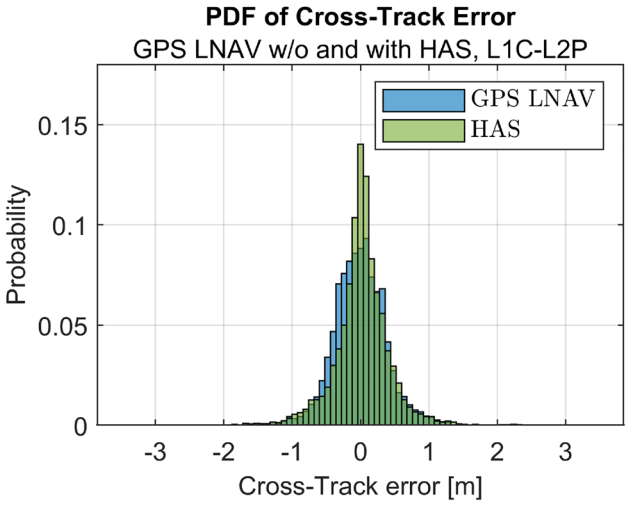


Fig. 9 Improvement of orbit errors when applying HAS, in particular the figure shows PDF of GPS Cross-Track error without (blue) and with HAS (green)

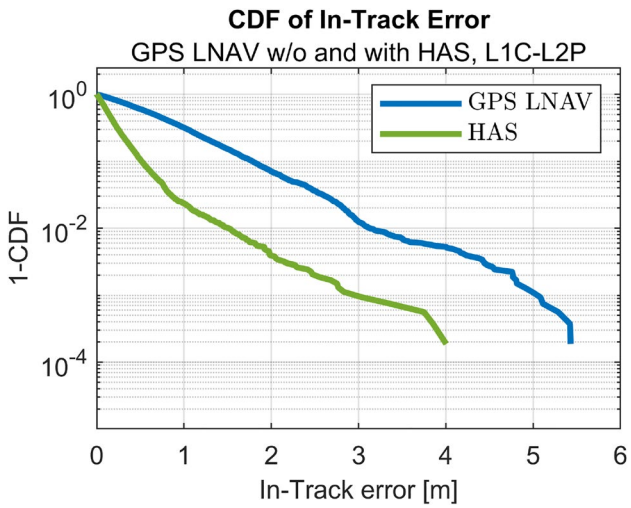


Fig. 8 Improvement of orbit errors when applying HAS, in particular the figure shows 1-CDF of GPS ln-Track error without (blue) and with HAS (green)

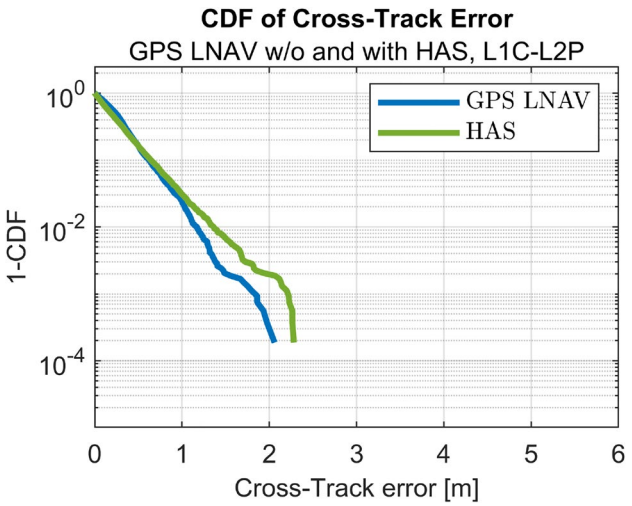


Fig. 10 Improvement of orbit errors when applying HAS, in particular the figure shows 1-CDF of GPS Cross-Track error without (blue) and with HAS (green)

most significant reduction was obtained for the Radial component, the one mostly impacting on the final ranging error. The HAS error distributions are closer to Gaussian distributions with respect not corrected distributions, as it appears in the reduction of the mean value and in the improvement of the symmetry of the PDFs. This aspect is important when optimizing the bounding of the errors in the integrity solutions while still ensuring high availability (Langel et al. 2021; Crespillo et al. 2023; Gallon et al. 2022) and while considering the implications on the computational load (Blanch et al. 2012; Gunning et al. 2018).

Figures 7, 8, 9, 10, 11, and 12 show the same effect on the GPS satellites. The broadcast errors are larger than in the Galileo case due to the longer update interval of the GPS message (2 h) compared to the Galileo ones (down to 10 min). The reduction of the errors and the difference with respect to a Gaussian distribution are confirmed in particularly for the In-Track component. In the GPS case the availability of the HAS corrections was reduced, and the minimum probability represented was 2×10^{-4}.

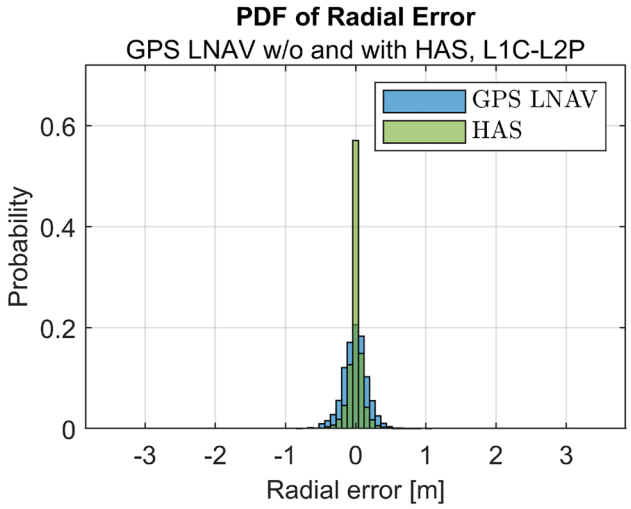


Fig. 11 Improvement of orbit errors when applying HAS, in particular the figure shows PDF of GPS Radial error without (blue) and with HAS (green)

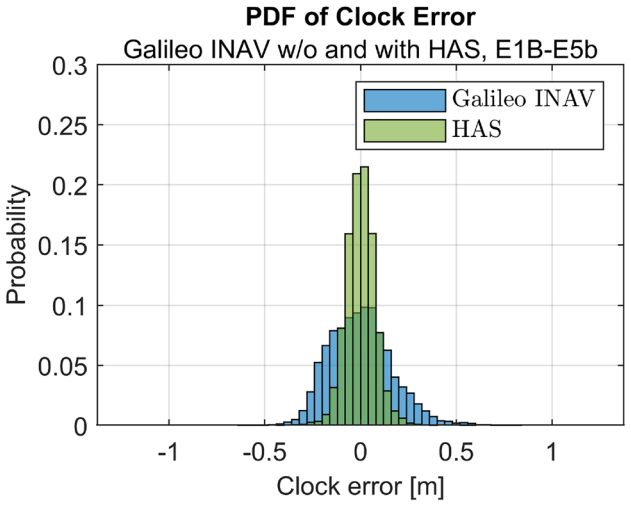


Fig. 13 Improvement of clock errors when applying HAS, in particular the figure shows the PDF of Galileo Clock error without (blue) and with HAS (green)

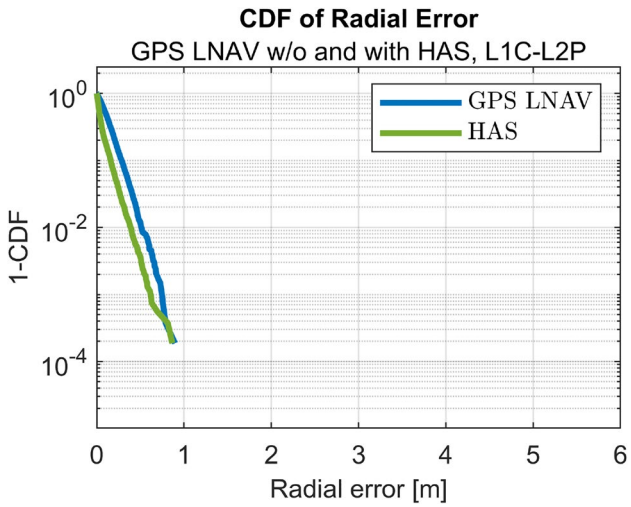


Fig. 12 Improvement of orbit errors when applying HAS, in particular the figure shows 1-CDF of GPS Radial error without (blue) and with HAS (green)

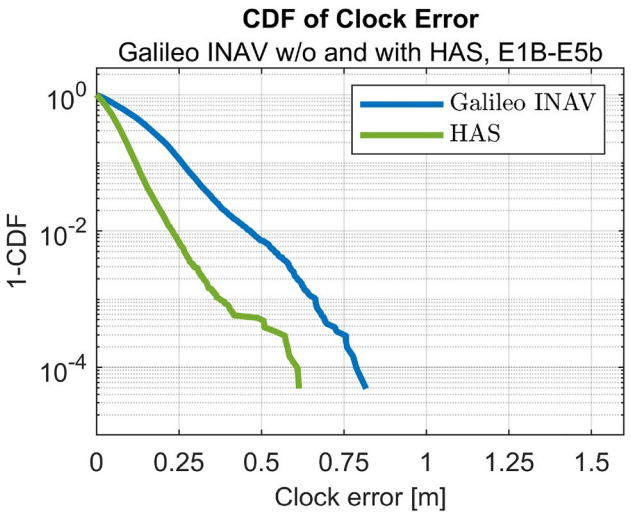


Fig. 14 Improvement of clock errors when applying HAS, in particular the figure shows the 1-CDF of Galileo Clock error without (blue) and with HAS (green)

Satellite clock error

This section shows the characterization of the clock error component. Figures 13, 14, 15, and 16 show the PDF (left) and the one-side CDF (right) for Galileo I/NAV (top) and for GPS LNAV (bottom). Similarly, to the satellite orbit case, the clock errors are significantly reduced when HAS corrections are applied. For Galileo the error reduced by a factor 2.13 and for GPS by a factor 1.3. The distributions are closer to Gaussian ones with reduced mean values and an improved symmetry. Since the clock performance is highly dependent on the clock type, especially for GPS, a specific analysis on the clock error separated for each clock type was performed (Fig. 17).

There are three main types of space-qualified atomic clocks used in GPS and Galileo: Rubidium or Rubidium Atomic Frequency Standard (Rb or RAFS), Cesium (Cs), or passive Hydrogen masers (PHMs). GPS satellites have been equipped with several combinations of clocks. GPS Block II/IIA carried two Cs and two Rb clocks, Blocks IIR and IIR-M contained three Rb clocks, and Block IIF carried two Rb and one Cs clock. Galileo satellites, on the other hand, use PHMs or RAFS as primary clocks, depending on the satellite, and as shown in the GSC website (European

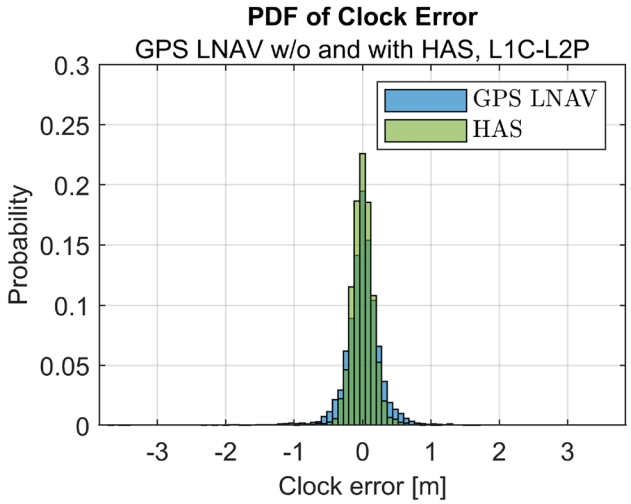


Fig. 15 Improvement of clock errors when applying HAS, in particular the figure shows the PDF of GPS Clock error without (blue) and with HAS (green)

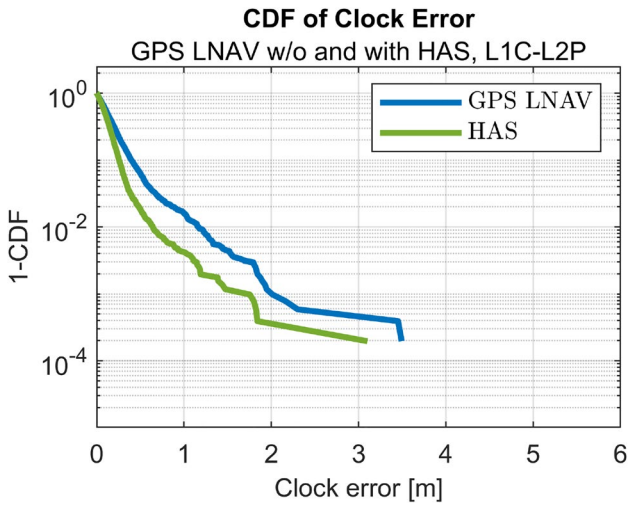


Fig. 16 Improvement of clock errors when applying HAS, in particular the figure shows the 1-CDF of GPS Clock error without (blue) and with HAS (green)

Union Space Program Agency 2023a; b). It has been shown that the type of GPS clock plays an important role on the accuracy of the ranging error since Cs clocks are in general less stable and accurate than Rb ones. Most recent and modern GPS satellites have Rb clocks in use, and it is not possible to separate the types of clocks by selecting the satellite block. The Navigation Center (NAVCEN) of the United States Coast Guard from the US Department of Homeland Security provides information on the type of clock active on each satellite, and this information was used to separate the characterization of Rb and Cs types. Over the period considered Cs clocks were operational on GPS SVN 65—PRN

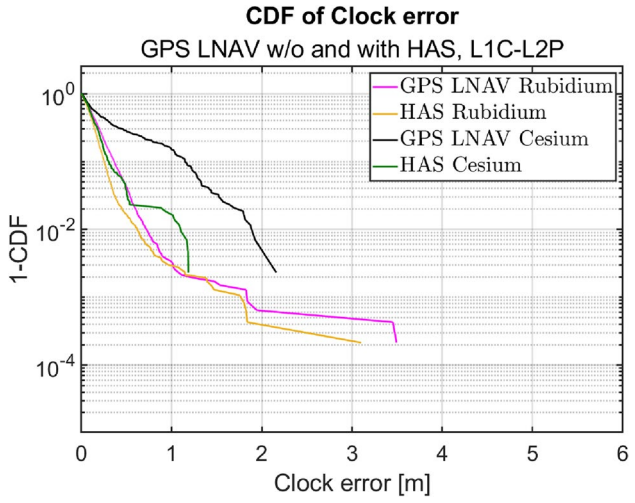


Fig. 17 Differences of HAS correction performance for different GPS clock types, in particular the figure shows the Rubidium and Cesium Clock error for GPS LNAV without and with HAS

24 (Block IIF) and GPS 72—SVN 8 (Block IIF), while all the other satellites had Rb clocks.

Figure 17 shows that the ranging errors of the Rb clocks are smaller than the Cs ones for the broadcast LNAV message (magenta and black, respectively). The HAS corrections improved the Cs error thanks to the high update rate of the clock corrections: the residual mean value is significantly smaller, and the root-mean-square is reduced by a factor of 2.6. The improvement is observed also for the Rb error (factor 1.3) particularly in the distribution tails.

Satellite signal in space error (SISE)

After the analysis of the single orbit and clock components, this section presents their combination in the ranging domain. This step highlights the real impact on the user since not all the components have the same effect (typically radial and clock are the most impacting ones). The error statistics for Galileo and GPS with and without HAS corrections are presented.

The error statistics for Galileo and GPS with and without HAS corrections are then presented. Figures 18, 19, 20, and 21 show the PDF and one minus CDF of the absolute value of the SISE for Galileo and GPS without (blue) and with HAS corrections (green). The density function was provided for ranging error without sign which is not relevant for the effect of the error on the user. The results confirm the behavior observed on the single error components. The errors are reduced by a factor 1.6 for Galileo and 1.4 for GPS, the distributions are closer to Gaussian ones, and the mitigation of the error on the tails, particularly for the GPS case, is confirmed.

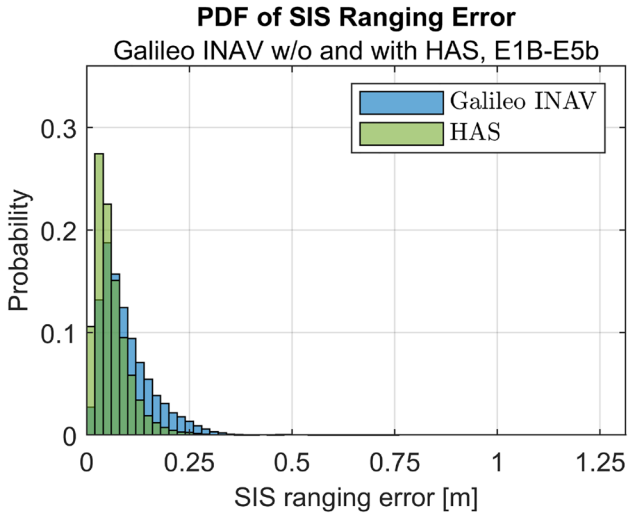


Fig. 18 Improvement of SIS errors when applying HAS, in particular the figure shows the One-side PDF of Galileo SISE without (blue) and with HAS (green)

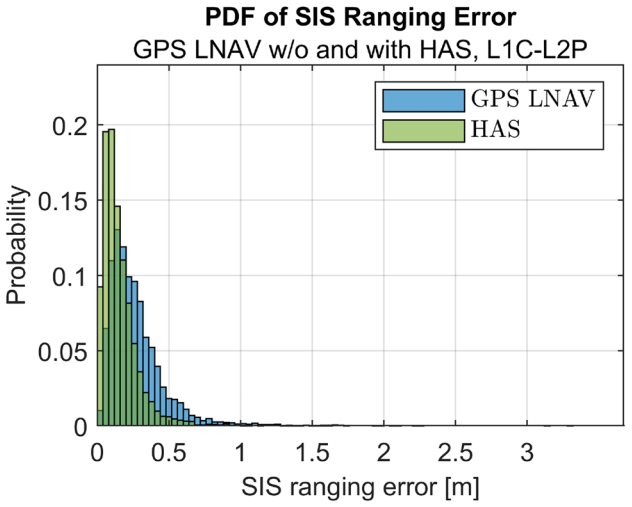


Fig. 20 Improvement of SIS errors when applying HAS, in particular the figure shows the One-side PDF of GPS SISE without (blue) and with HAS (green)

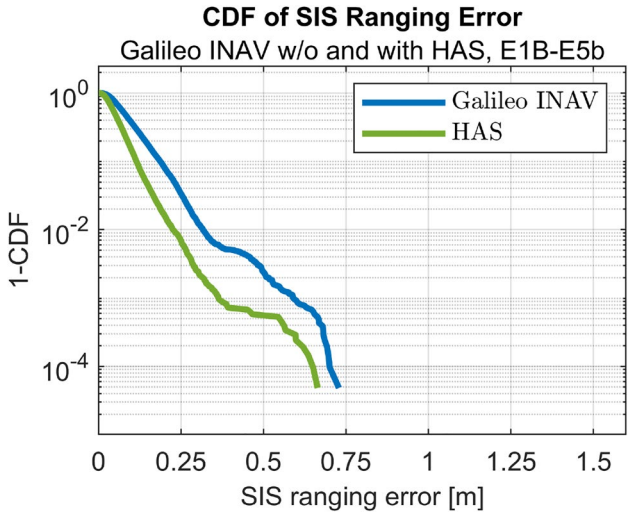


Fig. 19 Improvement of SIS errors when applying HAS, in particular the figure shows the 1-CDF of Galileo SISE without (blue) and with HAS (green)

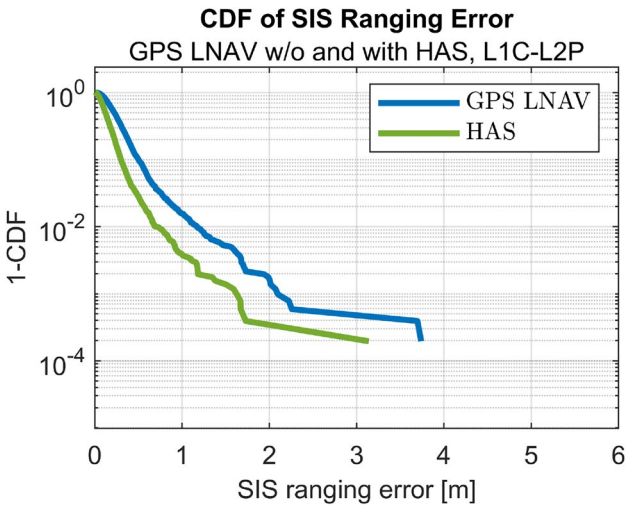


Fig. 21 Improvement of SIS errors when applying HAS, in particular the figure shows the 1-CDF of GPS SISE without (blue) and with HAS (green)

Tables 1 and 2 summarize the previous results for the different components and for the two constellations. It shows the overall improvement obtained by a user applying HAS corrections. The most impacting components, Clock and Radial, are reduced by a factor between 2 and 3.5 for Galileo and between 1.2 and 1.5 for GPS leading to a reduction factor of circa 1.5 in the SISEs. Overall the improvement of the performance can be appreciated for both GPS and Galileo and in particular for the RMS.

Satellite group delays and biases

This section describes the characterization of the group delay and code biases affecting the ranging errors. For Galileo, the I/NAV BGD and for GPS the LNAV TGD errors were compared to the corresponding HAS code biases. Statistical analyses similar to previous ones were performed.

Figures 22, 23, 24, and 25 and Table 3 show the results obtained on the bias characterizations. The biases were reduced by a factor of 2 circa for both Galileo and GPS. The

Table 1 Galileo ranging error statistics (m)

Galileo (m)	In-track		Cross-track		Radial		Clock		SISE	
	Mean	RMS	Mean	RMS	Mean	RMS	Mean	RMS	Mean	RMS
I/NAV	0.022	0.250	0.019	0.173	0.005	0.116	0.001	0.164	0.004	0.120
I/NAV + HAS	0.023	0.129	0.013	0.142	0.000	0.034	0.000	0.077	0.000	0.077

Table 2 GPS ranging error statistics (m)

GPS (m)	In-track		Cross-track		Radial		Clock		SISE	
	Mean	RMS	Mean	RMS	Mean	RMS	Mean	RMS	Mean	RMS
LNAV	0.081	1.108	0.012	0.390	0.008	0.175	0.001	0.297	0.003	0.361
LNAV + HAS	0.032	0.380	0.022	0.403	0.000	0.102	0.000	0.195	0.001	0.223

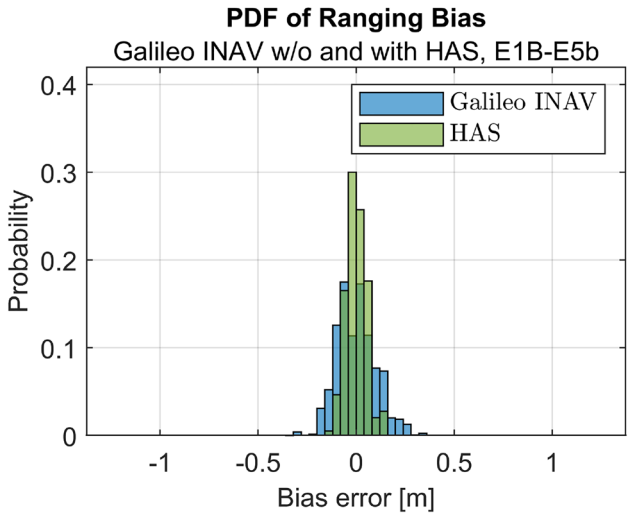


Fig. 22 Improvement of bias errors when applying HAS, in particular the figure shows the PDF of Galileo Bias error without (blue) and with HAS (green)

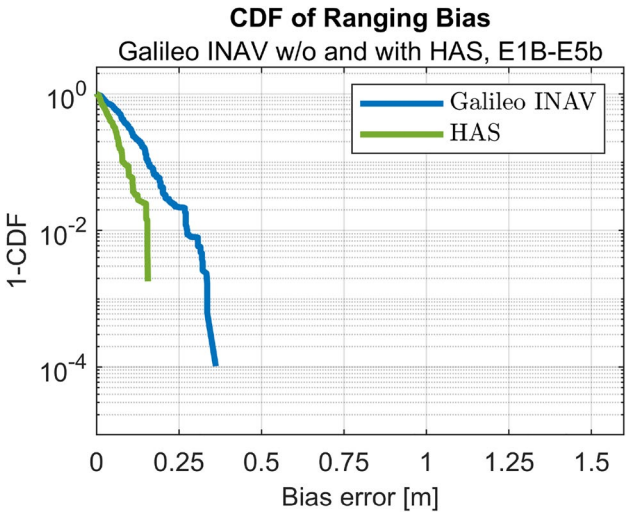


Fig. 23 Improvement of bias errors when applying HAS, in particular the figure shows the 1-CDF of Galileo Bias error without (blue) and with HAS (green)

parameters correcting these delays have different update rates: BGDs and TGDs are updated daily or even over several days, while HAS biases have 50-s update intervals. The refresh rate of the message does not imply that the numeric values are updated at each refresh of the message. This aspect is reflected in the different number of samples available for the CDF statistics and explains the different probabilities reached in the one-side CDFs. The plots show distributions closer to Gaussian ones especially in the GPS case where different satellite blocks can have different biases. Remarkable is the reduction of the mean value, particularly in the GPS case. In Table 3 it is observed a reduction of more than 50% on both constellations.

Correction and mitigation of anomalous ranging errors

Although HAS service does not provide an integrity commitment, safety–critical users may take benefit by exploiting it in evolutions of receiver autonomous integrity monitoring algorithm (RAIM) (Blanch et al. 2012; Gunning et al. 2018; Crespillo et al. 2023). Thanks to the high update rate of the corrections, their real-time dissemination, and the possibility to exclude satellites from the service, HAS is particularly beneficial to users in case of large ranging errors. Galileo HAS can correct the errors, mitigate their effects, reduce the time over which the user is exposed to the anomaly and inform that the satellite shall be excluded. These characteristics are interesting for receivers in critical applications which need to maximize

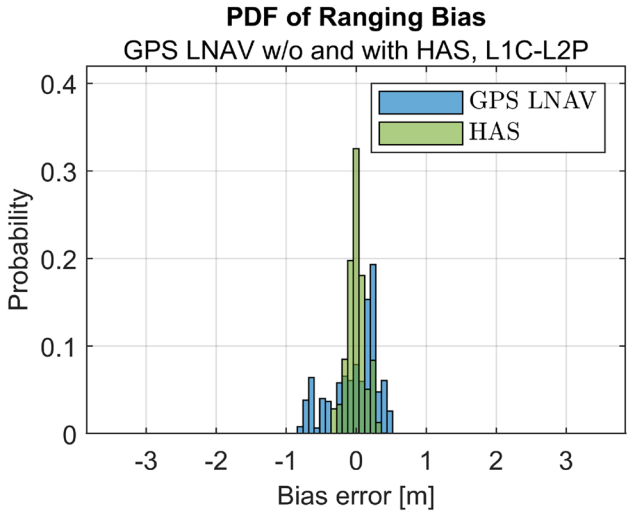


Fig. 24 Improvement of bias errors when applying HAS, in particular the figure shows the PDF of GPS Bias error without (blue) and with HAS (green)

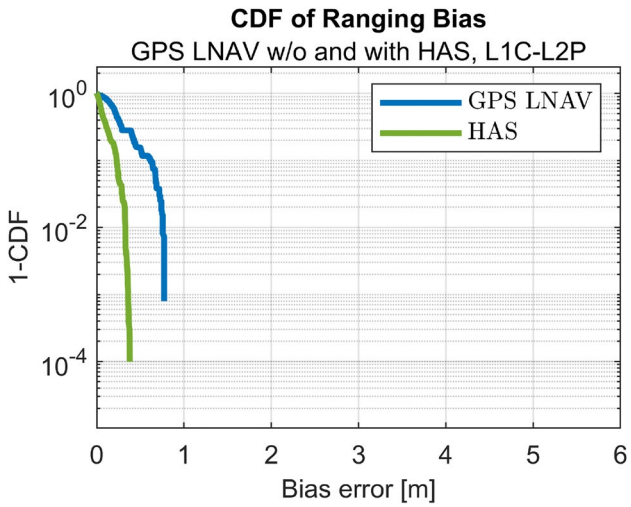


Fig. 25 Improvement of bias errors when applying HAS, in particular the figure shows the 1-CDF of GPS Bias error without (blue) and with HAS (green)

Table 3 Galileo and GPS code bias error statistics (m)

Group delay bias (m)	Galileo RMS	GPS RMS
Brdc	0.102	0.334
Brdc + HAS	0.054	0.126

their robustness to anomalous ranging errors. This section describes the behavior of HAS in cases observed during the live signals characterization. It extends the work on the topic already initiated in (Martini et al. 2022a; b). Four cases are analyzed, coinciding with periods when the Galileo HAS SIS was on: three for Galileo E01-GSAT0210 on September 5, 2021, April 29, 2022, and August 31, 2022—the satellite is now out of service, and one for GPS SVN73-PRN10, on September 24, 2021.

The first case concerns an event occurred on September 5, 2021, on Galileo E01-GSAT0210. It is shown in Fig. 26 and time is expressed in UTC reference. The signals were nominal until 5:42:00 and then started drifting between 5:42:00 and 5:42:30, both on I/NAV and F/NAV messages. The I/NAV and F/NAV health status switched from healthy to unhealthy at 6:05:00 (green). As defined in the Galileo SDD (European Union Space Program Agency 2019), the health status of the satellite is obtained from the combination of the data validity status (DVS), the satellite health status (SHS), and the signal in space accuracy (SISA). When one of these parameters is set to unhealthy, the satellite is set to unhealthy. In this case, the SISA indicator was set to no accuracy prediction available (NAPA).

Later, a Galileo Service Notice was published indicating that the Galileo E01-GSAT0210 was affected by an "onboard issue" causing a rapid drift of the ranging error. The Galileo Service Centre also notified the users about this event with the NAGU #2021012. As clarified in the Service Notice, the event was notified in agreement with the Open Service commitment of 1-h exposure time.

HAS during the event. HAS corrections during the first minute followed the error ramp and thanks to their short update interval of 10 s they could well match the errors. The message includes a multiplier for the correction, between 1 and 4, which allowed to represent large ranging errors, as in this case. After more than one minute of following the error, HAS corrections were set to 'data not available' (value of − 10.2375 m) at 5:43:47. Therefore, a HAS user was exposed to the event only for an interval of 1 min and 17 s, during which the HAS correction followed the error.

A receiver applying a strict exclusion logic could exclude the satellite in the first clock correction update if the value suddenly raises from the typical decimeter-level values to several meters, as was the case here. In addition, the HAS data availability flag can be used to remove satellites with degraded performance, improving the receiver fault detection and exclusion. These characteristics can be exploited by PPP algorithms but also by SPP ones to increase receiver robustness. Methods for the receiver processing to exploit HAS benefits for safety critical applications were presented in Martini et al. (2022a; b).

In the second case, HAS clock corrections mitigated a clock ramp observed again on Galileo E01-GSAT0210 on April 29, 2022 (Fig. 27). Also in this case, the clock error started drifting (blue) after 00:58:30, and the signal was set to unhealthy in the I/NAV message at 1:35:00. A NAGU disabling the satellite was issued some hours later (European Union Space Program Agency 2022a; b, c). At the time

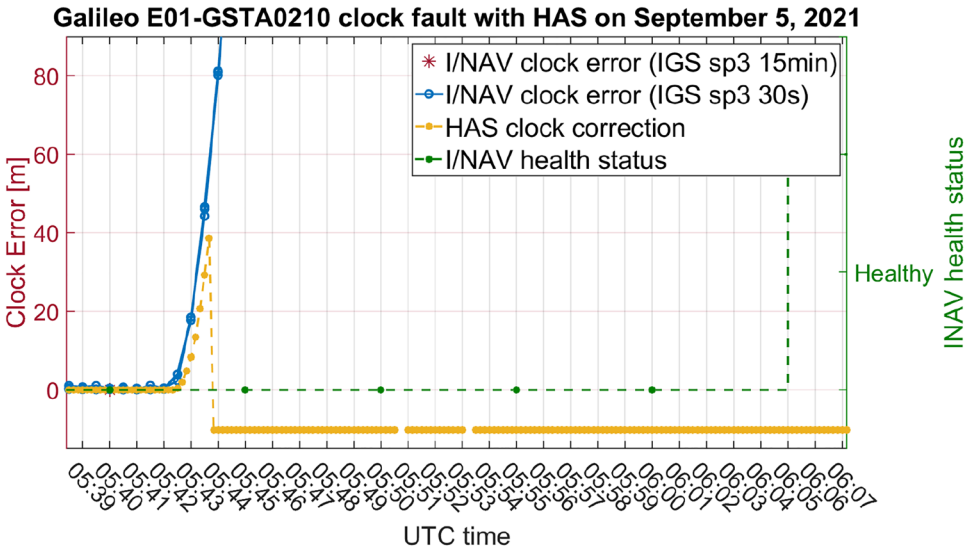


Fig. 26 HAS clock corrections (orange) on September 5, 2021, during Galileo E01-GSAT02010 clock degradation (blue) indicated by the I/NAV health status (green). HAS corrected the errors and then informed the user in less than 2 min that the satellite could not be used by switching to 'data not available' (− 10.2375 m)

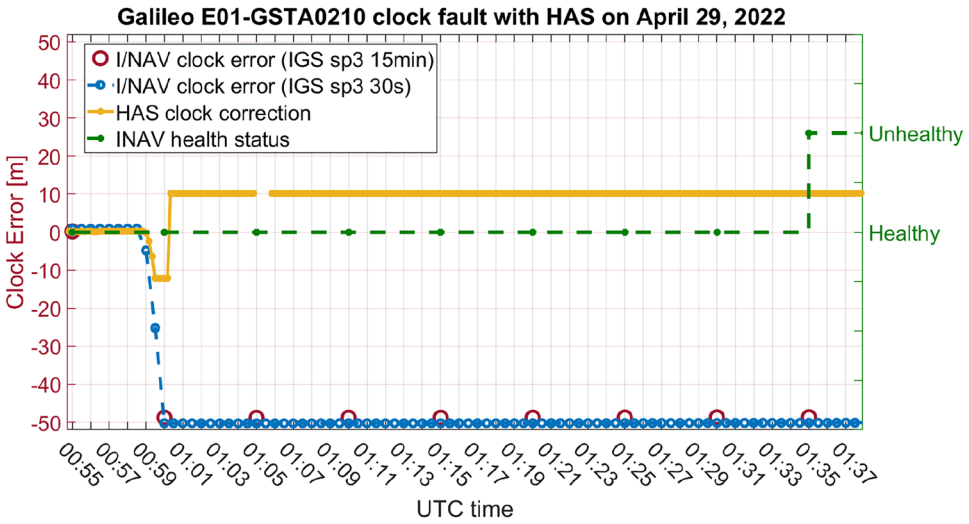


Fig. 27 HAS clock corrections (orange) on April 29, 2022, during Galileo E01-GSAT02010 clock degradation (blue) indicated by the I/NAV health status (green). HAS first corrected the error and then informed the user within few minutes by switching to 'data shall not be used' (10.2375 m)

of the event, the HAS correction (orange) promptly started following the true clock error. After less than a minute, the corrections were set to 'data shall not be used' (value of 10.2375 m) informing the user that the satellite needed to be excluded from the solution computation. It was observed that the corrections remained stable to a constant value after 30 s from the start of the ramp although the error continued growing. This delay in the switching point was due to a two-step process between the HAS generation and the flagging mechanism which was present in a previous version of the high accuracy data generator (HADG) element of the HAS. In current versions after Initial Service this two-step approach is not present, and this behavior has not been and should not be observed anymore.

Figure 28 shows the third case analyzed, where the HAS corrections followed the effect of an anomalous clock error again on Galileo E01-GSAT0210 on August 31, 2022. Also, in this case applying HAS corrected the error with a delay of seconds. Then, after some minutes, it sets the correction to 'data not available' for another 14 min, after which the correction is again transmitted until the satellite is declared unhealthy in the I/NAV message after around 40 min from the fault onset (European Union Space Program Agency 2022a; b, c).

Finally, Fig. 29 shows a case in which the clock of the GPS SVN 73-PRN 10 (ID 11) drifted for some meters on September 24, 2021, after 11:00. In this case the health status was maintained as healthy for the GPS LNAV users for the whole event duration. HAS correction was set to 'data not available' for some minutes prior to the event. Then, when the drift started, HAS set the correction to 'data not available', with some instabilities before correcting the error again. As in previous cases, and even if HAS significantly reducing the exposure time to the error, we must note that this event occurred at the beginning of the HAS SIS testing, while the HADG was not fully tuned and HAS monitoring capabilities still not fully deployed.

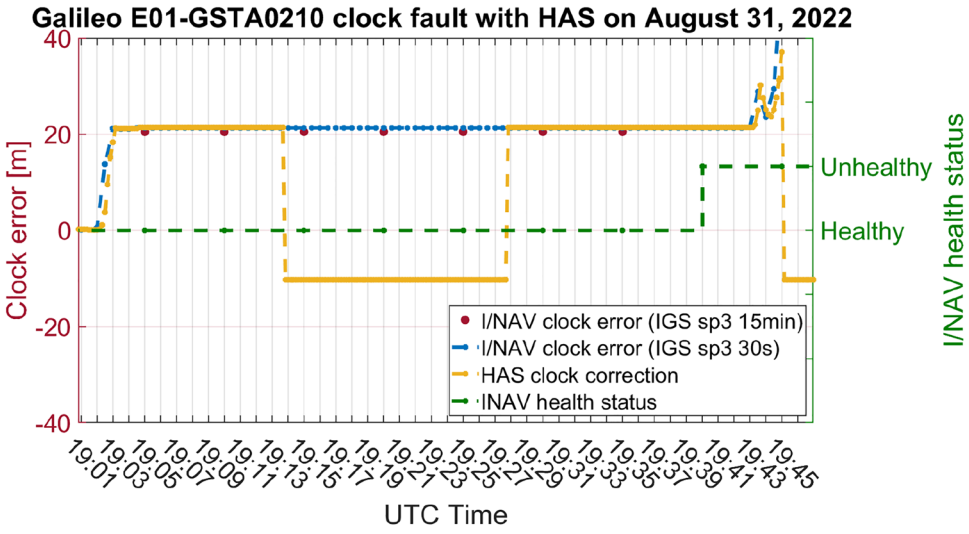


Fig. 28 HAS clock corrections (orange) on August 31, 2022, during Galileo E01-GSAT02010 clock degradation (blue) indicated by the I/NAV health status (green). HAS corrected the error and then switch temporarily to 'data not available' (– 10.2375)

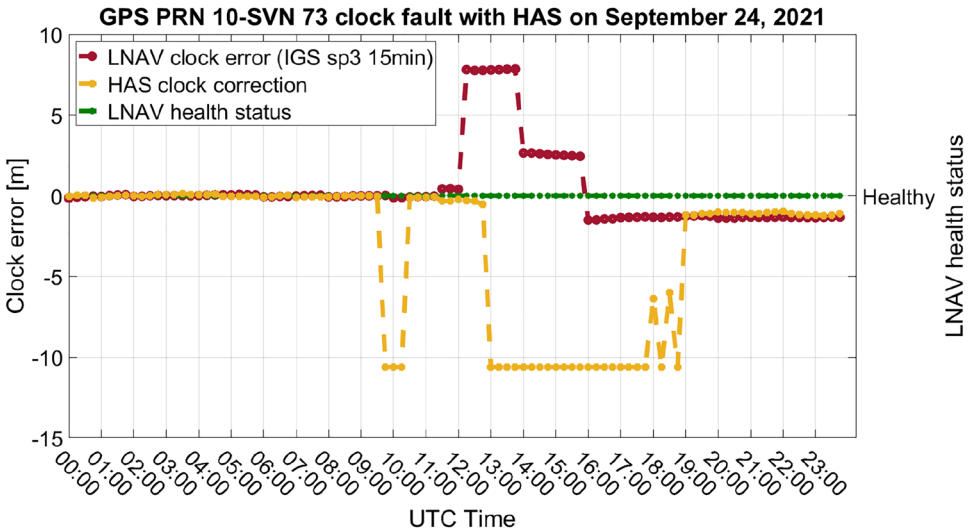


Fig. 29 HAS clock corrections (orange) on September 24, 2021, during GPS SVN 73-PRN 10 clock degradation (red) which was not indicated by the I/NAV health status (green). HAS corrected the error and informed the user that the satellite could not be used by switching to the value of – 10.2375

User positioning error

The characterization of the performance in the position domain was performed using a HAS user terminal (HAUT) receiver located at JRC and developed in the framework of a procurement of the European Union Agency for the Space Programme (EUSPA). User performance was analyzed in both static open sky and dynamic conditions. The reference data for the static case were the precise position of the antenna located on the roof of the JRC building. Data were collected on February 24, 2023, and the HAS PPP solution after convergence was compared to a standard, code-based SPP (single point positioning) solution, as displayed in Fig. 30. The SPP was assessed using a ionofree dual-frequency combination using GPS + Galileo and the Klobuchar model accordingly to aviation RTCA MOPS 229D standard. A carrier smoothing with 100 s was also applied to reduce the noise impact. The HAS solution was measured after convergence, using a GPS + Galileo dual-frequency float solution using L1 and L5 signals and ionospheric-free combination. Most of the solutions were performed without ambiguity fixes. More details can be found in (Pintor et al. 2022).

The HAS solution has an accuracy below 3.6 cm RMS in the horizontal dimension and below 7.6 cm in the vertical ones, much better than SPP with an accuracy below 72 cm in the horizontal dimension and 155.3 cm in the vertical ones. The legend of the plot displays the mean and the standard deviation of the corresponding accuracies. The scatter plot of the horizontal position error displayed in the bottom left of Fig. 30 shows that the standard deviation is reduced from 87.5 to 3.6 cm. The one-side CDF displayed in the bottom

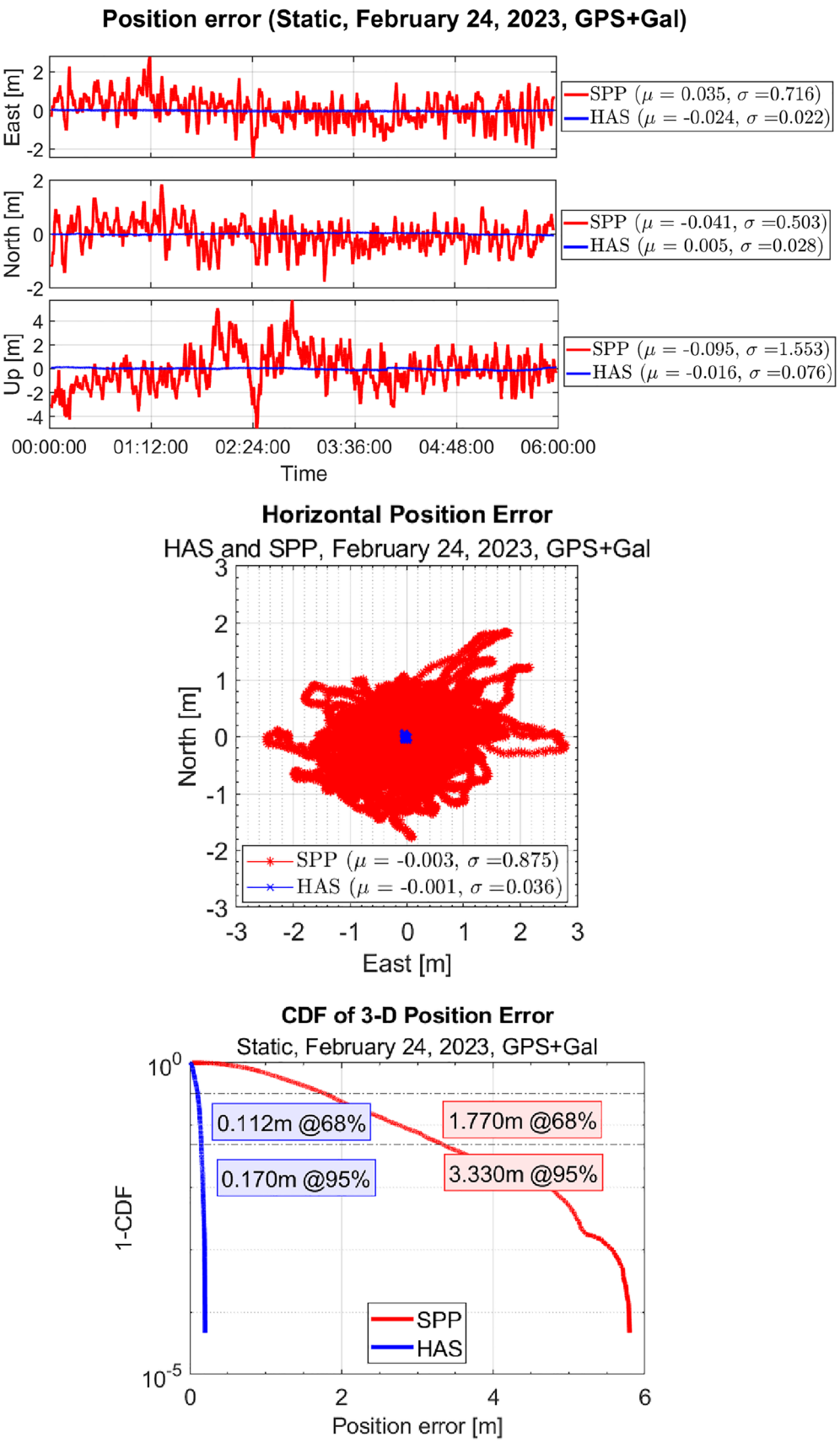


Fig. 30 For a static user comparison of HAS PPP (blue) and SPP (red) solutions with GPS + Gal signals. The time series of the east, north, up position error components over a representative interval of the data campaign (top), scatter plot of the horizontal position error (middle) and one-side CDF of the 3D position error (bottom)

right highlights the behavior for the distribution tails: the HAS PPP solution remains always below the 20 cm, while the SPP ones exceeded 5.8 m. The convergence time was analyzed performing 4 consecutive cold starts at a distance in time of circa 1 h and half. The convergence was considered reached when both components were below, respectively, 20 cm and 40 cm. We observed a typical convergence time of 15 min.

For the dynamic test, the receiver was mounted in a van with an antenna provided by the Fraunhofer Institute for Integrated Circuits. The van performed an automotive data collection in the JRC campus on December 20, 2022 (Fig. 31). The trajectory followed by the van was performed in a harsh environment with several trees and buildings to test the receiver in challenging conditions (Fig. 32). The reference trajectory was obtained through a postprocessing RTK solution provided by Novatel Inertial Explorer software.

The comparison between the HAS PPP and the SPP solution in the dynamic case is displayed in Fig. 33. As previously described the data collection was performed with a van driving through the JRC campus in a challenging environment, therefore the receiver suffered several data gaps which required restarting of the filters and consequent reconvergence. When the receiver converged and provided the HAS solution, the performance confirmed the significant improvement of the east, north, and up error component with respect to the SPP solution as displayed in Fig. 33. The standard deviation reduced from circa 68–19 cm (top). The scatter plot and the one-side CDF show that the horizontal position error reduced from 96.4 to 26.7 cm and the 3D error from 111 to 33.1 cm. Also in this case the distribution tails are less heavy with a 95% of the 3D errors below 263.8 cm for SPP and below 54.1 cm for HAS.

Conclusions

The Galileo Program announced on January 24, 2023, the Initial Service of the Galileo High Accuracy Service, a free-of-charge PPP service aiming at worldwide coverage transmitted on E6 signals and through an internet connection. This paper has shown the accuracy of the HAS orb, clock, and bias products, the HAS corrections behavior in case of real satellite anomalies, and some user position results in static and dynamic environments.

HAS products were evaluated just after service declaration. The accuracy of HAS-corrected orbits, clocks, and SISE was evaluated and compared to the Galileo I/NAV and GPS LNAV broadcast navigation messages. Improvements were particularly relevant for the radial component of the orbital error and the clock component, up to a factor of 3 for Galileo. The SISE was analytically computed based on the orbit errors, showing also relevant improvements, which



Fig. 31 JRC van and its trajectory during the automotive experimentation campaign performed on December 20, 2022, @EC JRC campus (Ispra, Italy)



Fig. 32 JRC campus environment with tree canopy and other obstructions

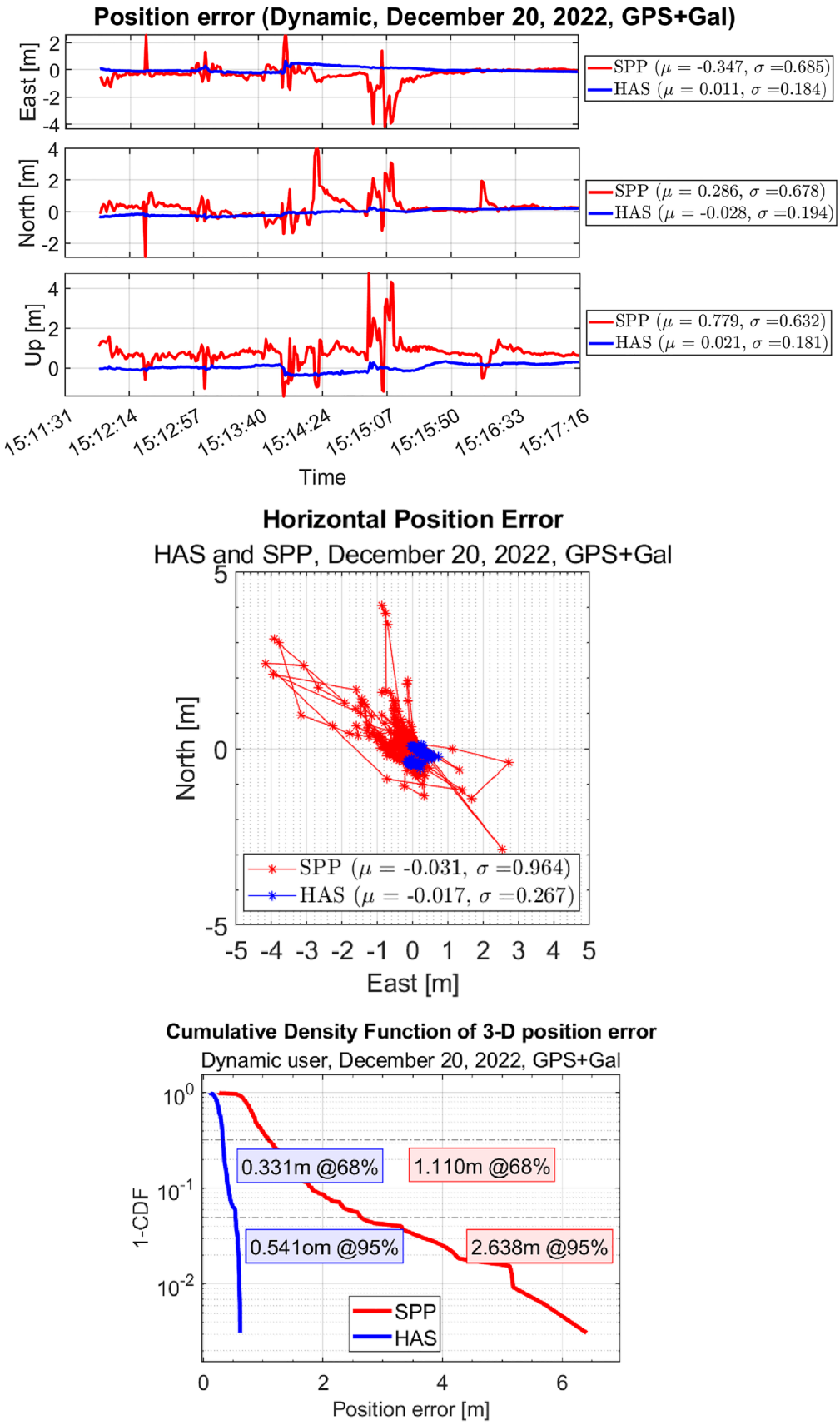


Fig. 33 For a dynamic user comparison of HAS PPP (blue) and SPP (red) solutions with GPS + Gal signals. The time series of the east, north, up position error components (top), scatter plot of the horizontal position error (middle) and one-side CDF of the 3D position error (bottom)

included also the tails of the error distributions, measured down to probabilities below 10–4. Code biases were also compared, showing similar improvement.

The behavior of HAS during four satellite anomalies between September 2021 and August 2022 was also analyzed. These included three events of Galileo satellite E01-GSAT0210 (not set as 'not usable') and one event in GPS SVN 73-PRN 10, all showing clock errors of several meters. In all Galileo events, HAS corrections followed the clock error with a short delay, driven by the 10-s clock update rate in the HAS message, before setting the correction to 'data not available' or 'satellite shall not be used'. Only in the case of GPS the corrections delay was longer than expected, which is attributed to the early testing stages of HAS. Users willing to apply a strict satellite exclusion logic may use the magnitude or variation the clock corrections before the satellite is flagged by HAS as not available or unusable, reducing exposure time even further.

Finally, the user positioning performance was evaluated both static and dynamic conditions. The static case used data from a high-grade antenna at JRC, Ispra, Italy, in open sky conditions. Results showed an accuracy after convergence below 3 cm in both horizontal components, and below 8 cm in the vertical component, both at 1-sigma. The dynamic test was based on a HAS receiver mounted on a van driving around JRC premises, under tree canopy and other obstructions. Even in these conditions, results showed a horizontal positioning error of 26.7 cm, 1-sigma, significantly better than the standard, code-based position obtained from a commercial, state-of-the-art receiver, of about 1 m, 1-sigma. Further characterization work will include more dynamic and HAS convergence testing under different user modes and conditions.

Acknowledgements This study was funded by the European Commission Joint Research Center, Ispra, Italy.

Author contributions All authors contributed to the study conception and design. Material preparation, data collection, and analysis were performed by IM. The first draft of the manuscript was written by IM, and all authors commented on previous versions of the manuscript. All authors read and approved the manuscript.

Data availability The data used for the characterization of the HAS accuracy performances were available on the IGS webservers at the following archives: For GPS broadcast message https://cddis.nasa.gov/archive/gnss/data/daily/. For GPS reference products https://cddis.nasa.gov/archive/gnss/products/. For GPS Inter-signals Correction https://cddis.nasa.gov/archive/gnss/data/daily/. For Galileo broadcast message https://cddis.nasa.gov/archive/gnss/data/daily/. For Galileo reference products https://cddis.nasa.gov/archive/gnss/products/. For satellite Differential Code Biases https://cddis.nasa.gov/archive/gnss/products/bias/. The Galileo HAS data were collected at European Commission, Joint Research Center, in the testing laboratory of the Galileo Sector Unit E.2, Technologies for Space, Security, and Connectivity.

Declarations

Conflict of interest All authors certify that they have no affiliations with or involvement in any organization or entity with any financial interest or non-financial interest in the subject matter or materials discussed in this manuscript.

Open Access This article is licensed under a Creative Commons Attribution 4.0 International License, which permits use, sharing, adaptation, distribution and reproduction in any medium or format, as long as you give appropriate credit to the original author(s) and the source, provide a link to the Creative Commons licence, and indicate if changes were made. The images or other third party material in this article are included in the article's Creative Commons licence, unless indicated otherwise in a credit line to the material. If material is not included in the article's Creative Commons licence and your intended use is not permitted by statutory regulation or exceeds the permitted use, you will need to obtain permission directly from the copyright holder. To view a copy of this licence, visit http://creativecommons.org/licenses/by/4.0/.

References

Blanch J, et al (2012) Advanced RAIM user algorithm description: integrity support message processing, fault detection, exclusion, and protection level calculation. In: Proceedings of ION GNSS+ 2012, Institute of Navigation, September 17–21, 2012. Nashville Convention Center Nashville, Tennessee, pp 2828–2849

Crespillo OG, Langel S, Joerger M (2020) Tight bounds for uncertain time-correlated errors with gauss-markov structure in kalman filtering. IEEE Trans Aerosp Electron Syst. https://doi.org/10.48550/arXiv.2009.09495

European Union Space Program Agency (EUSPA) (2019) Galileo open service—service definition document, issue 1.1. https://www.gsc-europa.eu/sites/default/files/sites/all/files/Galileo-OS-SDD_v1.1.pdf

European Union Space Program Agency (EUSPA) (2020) Information note on Galileo high accuracy service. https://www.gsc-europa.eu/sites/default/files/sites/all/files/Galileo_HAS_Info_Note.pdf

European Union Space Program Agency (EUSPA) (2022a) Galileo high accuracy service signal-in-space interface control document (HAS SIS ICD). https://www.gsc-europa.eu/sites/default/files/sites/all/files/Galileo_HAS_SIS_ICD_v1.0.pdf

European Union Space Program Agency (EUSPA) (2022b) GSC notice advisory to Galileo users. https://www.gsc-europa.eu/notice-advisory-to-galileo-users-nagu-2022015

European Union Space Program Agency (EUSPA) (2022c) Notice advisory to Galileo users. https://www.gsc-europa.eu/notice-advisory-to-galileo-users-nagu-2022035

European Union Space Program Agency (EUSPA) (2023a) Galileo constellation information. https://www.gsc-europa.eu/system-service-status/constellation-information

European Union Space Program Agency (EUSPA) (2023b) Galileo high accuracy service registration. https://www.gsc-europa.eu/galileo/services/galileo-high-accuracy-service-has/internet-data-distribution-registration-form

Fernandez-Hernandez I, Senni T, Borio D, Vecchione G (2020) High-Parity vertical Reed Solomon codes for long GNSS high accuracy messages. Navig J Inst Navig 27:365–378

Fernandez-Hernandez I et al (2022) Galileo high accuracy service: initial definition and performance. GPS Solut 26:65

Gallon E, Joerger M, Pervan B (2022) Robust modeling of GNSS orbit and clock error dynamics. J Navig 69(4). https://doi.org/10.33012/navi.539

Gunning K, et al (2018) Design and evaluation of integrity algorithms for PPP in kinematic applications. In: Proceedings of ION GNSS+2018, Institute of Navigation, Miami, Florida, September 2018, pp 1910–1939. https://doi.org/10.33012/2018.15972

Horst O, et al (2022) HASlib: an open-source decoder for the Galileo high accuracy service. In: Proceedings of ION GNSS+2022, Institute of Navigation, Long Beach, California, January 2022, pp 2625–2633. https://doi.org/10.33012/2022.18261

Langel S, Crespillo OG, Joerger M (2021) Overbounding the effect of uncertain Gauss–Markov noise in Kalman filtering. J Navig 68(2):259–276

Martini I, Susi M, Fernandez-Hernandez I (2022a) PPP and Galileo high accuracy service with satellite selection strategies for kinematic applications. In: Proceedings of ION GNSS+2022, Institute of Navigation, Long Beach, California, January 2022, pp 667–682. https://doi.org/10.33012/2022.18261

Martini I, et al (2022b) Satellite anomaly detection with PPP corrections: a case study with Galileo's high accuracy service. In: Proceedings of ION GNSS+2022, Institute of Navigation, Long Beach, California, January 2022, pp 1246–1262. https://doi.org/10.33012/2022.18261

Montenbruck O, Steigenberger P, Hauschild A (2018) Multi-GNSS signal-in-space range error assessment—methodology and results. Adv Space Res 61(12):3020–3038

Pintor P, et al (2022) Galileo high accuracy service (HAS) algorithm and receiver development and testing. In: Proceedings of the ION GNSS+ 2022, Institute of Navigation, Denver, Colorado, September 2022, pp 836–851. https://doi.org/10.33012/2022.18462

RTCM Standard 10403.3, May 20 (2021) RTCM differenctial GNSS (global navigation satellite systems) services, version 3 with amendment 1

RTCM Standard 10410.1, January 12 (2021) Standard for networked transport of RTCM via internet protocol (Ntrip) version 2.0 with amendment 2

Teunissen P, Montenbruck O (2017) Handbook of global navigation satellite systems. Springer, Berlin

Publisher's Note Springer Nature remains neutral with regard to jurisdictional claims in published maps and institutional affiliations.



Ilaria Martini worked as leader of research group on GNSS evolution at the German Aerospace Center, and then, she was technical advisor at the European Commission on GNSS R&D and standardization activities for safety critical applications. She is currently Principal Research Engineer at u-blox leading the technical R&D activities on integrity.



Melania Susi holds a Ph.D. from the University of Nottingham where she was a Marie Curie fellow. Currently she works at the Joint Research Centre of the European Commission in Galileo high accuracy, among other activities.



Luca Cucchi is currently serving as Scientific/Technical Officer at the Joint Research Centre (JRC) of the European Commission in Ispra, Italy, in the field of GNSS navigation. Under his position Luca provides engineering support to European Commission and EUSPA. He received an MSc in Telecommunication Engineering from University of Pisa in 2005, and he worked in private sector as radio navigation engineer from 2005 to 2019.



Ignacio Fernandez-Hernandez is responsible for Galileo high accuracy and authentication services at the EC, DG DEFIS, where he has led the design and development of OSNMA and HAS. He is an electronics engineer by ICAI (Madrid) and holds a Ph.D. degree by Aalborg University.